Talanta 104 (2013) 103–108

Contents lists available at SciVerse ScienceDirect

Talanta

journal homepage: www.elsevier.com/locate/talanta

Towards the fabrication of a label-free amperometric immunosensor using SWNTs for direct detection of paraoxon

Guozhen Liu [a,*], Dandan Song [a], FengJuan Chen [b]

[a] Key Laboratory of Pesticide and Chemical Biology of Ministry of Education, College of Chemistry, Central China Normal University, Wuhan 430079, PR China
[b] Key Laboratory of Nonferrous Metals Chemistry and Resources Utilization of Gansu Province and College of Chemistry Chemical Engineering, Lanzhou University, Lanzhou 730000, PR China

ARTICLE INFO

Article history:
Received 9 August 2012
Received in revised form
9 November 2012
Accepted 17 November 2012
Available online 23 November 2012

Keywords:
Immunosensor
SWNTs
Aryldiazonium salts
Detection of paraoxon

ABSTRACT

A label-free immunosensor based on SWNTs modified GC electrodes has been developed for the direct detection of paraoxon. Based on aryldiazonium salt chemistry, forest of SWNTs can be vertically aligned on mixed monolayers of aryldiazonium salt modified GC electrodes by C–C bonding, which provides an interface showing efficient electron transfer between biomolecules. PEG molecules were introduced to the interface to resist non-specific protein adsorption. Ferrocenedimethylamine (FDMA) was subsequently attached to the ends of SWNTs through the amide bonding followed by the attachment of epitope i.e., paraoxon hapten to which a paraoxon antibody would bind. This immunosensor shows good selectivity and high specificity to paraoxon, and is functional for the detection of paraoxon in both laboratory and field by a displacement assay. There is a linear relationship between electrochemical signal of FDMA and the concentration of paraoxon over the range of 2–2500 ppb with a lowest detected limit of 2 ppb in 0.1 M phosphate buffer at pH 7.0. The SWNTs based amperometric immunosensor provides an opportunity to develop the sensing system for on-site sensitive detection of a spectrum of insecticides.

1. Introduction

Organophosphorus compounds, such as paraoxon, are widely used as insecticides. The cellular mechanism of insecticidal action of the organophosphorus compounds involves inhibition of acetylcholine esterase, a key enzyme for nerve function. The common feature in the action of the enzyme is the hydrolysis of phosphate bonds in insecticides. Accidental exposure of humans and domestic animals to such insecticides results in a potentially lethal cholinergic poisoning. The organophosphorus based insecticides are potentially more toxic toward insects than chlorinated hydrocarbons. The relatively higher solubility (versus chlorinated compounds) of the organophosphorus based insecticides in water poses a threat to aquatic life unless they are hydrolyzed (the solubility of paraoxon in water is 2.40×10^6 ppb at 298 K) [1]. It is therefore essential to monitor the levels of these insecticides in industrial waste waters, in agriculture run-off, and in other environments.

In response to the need to detect organophosphorus based insecticides, a variety of sensors have been reported based on chromatographic, biological, or other techniques to separate, identify and/or quantify the insecticides [2–4]. Among these techniques, biological approaches afford rapid, specific, and sensitive detection as well as compatibility with miniaturized and portable devices. Because of strong inhibition and wide substrate specificity, acetylcholine esterase and phosphotriesterase are the popular enzymes used for biosensors for detection of this class of compounds. However, the inhibition reactions generally require long incubation time for sufficient sensitivity and long regeneration time of the inhibited enzyme necessary for reusing the sensors [5]. Due to the unique biocatalytic activity of organophosphorus hydrolase to a range of organophosphates, organophosphorus hydrolase based biosensors take steps further for the detection of organophosphorus compounds [6–8]. However, organophosphorus hydrolase based biosensors suffer from the serious interference problem due to the relatively high operating potential and poor selectivity of organophosphorus hydrolase [9].

Immunochemical techniques such as immunoassay based on the antibody–hapten reaction have lately gained a position as alternative and/or complementary methods for the analysis of agrochemicals because of their specificity, cost-effectiveness, and high sample throughput [10]. Electrochemical immunoassays in particular, are attractive for the detection of pesticides due to the high specificity by introducing the monoclonal antibody to the sensing interface [11]. The limitation of the immunoassays method involves the requirements of label process [12].

* Corresponding author Tel.: +86 27 6786 7535.
E-mail address: gzliu@mail.ccnu.edu.cn (G. Liu).

0039-9140/$ - see front matter © 2012 Elsevier B.V. All rights reserved.
http://dx.doi.org/10.1016/j.talanta.2012.11.039

Hu et al. have reported a label-free electrochemical immunosensor with paraoxon antibodies loaded on the gold nanoparticles to monitor the concentration of paraoxon in aqueous samples [13]. However, this immunosensor still suffers from the problem of poor selectivity and specificity to the target analyte paraoxon.

Vertical alignment of single walled carbon nanotubes (SWNTs) on surfaces offer new materials with interesting properties for future applications in electronic and electrochemical biosensors because of the high electron-transfer rate along the tube [14–16]. The most applied method to anchor SWNTs is perhaps based on the formation of amide bonds from the reaction between the amines located on the modified electrode and the carboxylic groups at the ends of side-wall defects of the nanotubes [17,18]. Highly ordered covalent anchoring of carbon nanotubes through C–C bonds binding on electrode surfaces modified with aryldiazonium salts is also reported [19]. The latter provides higher electron transfer rate due to the shorter insulating tethered layers at the interface.

In this work we aim to develop a label-free amperometric immunosensor based on SWNTs-aryldaizonium salt modified sensing interface for the detection of paraoxon (Scheme 1). Firstly, mixed monolayers of aryldiazonium salts were fabricated on GC substrate through aryldiazonium salt chemistry, which are expected to have stability advantages over those based on SAMs of alkanethiols on gold where the anchoring layer is simply chemisorbed to the surface [20]. Then vertically aligned SWNTs can be bonded on the surface through C–C binding, which is essential to the efficient electron transfer between the substrate and the target analyte. Mixed monolayers of diazonium salts also benefit the assembly of SWNTs to the surface [19]. To resist the non-specific protein adsorption, 2-(2-(2-(4-amino-phenoxy)-ethoxy)-ethoxy)-ethanol (PEG) molecules were modified to the wall of SWNTs. The SWNTs modified surface was then modified with the redox probe ferrocenedimethylamine (FDMA) and the epitope (paraoxon hapten), respectively. Finally, to increase the specificity of immunosensor the paraoxon monoclonal antibodies were introduced to the sensing interface. Binding of the antibody to the surface-bound epitope immerses the ferrocene in a protein medium. A consequence of this change in environment is the attenuation of electron transfer to the ferrocene due to the inaccessibility of a counterion. The PEG antifouling layer ensured the antibody only interacted with the interface when a specific biorecognition event occurred. Furthermore, the rigidity of SWNTs was essential to allow access of the antibody to the surface epitope without hindrance from the surface.

2. Materials and methods

2.1. Chemicals and Instruments

Sodium nitrite, potassium ferricyanide, hydrochloric acid, 4-phenylenediamine, aniline, *N*-hydroxysuccinimide (NHS), *N,N'*-dicyclohexylcarbodiimide (DCC), 1-ethyl-3-(3-dimethyl aminopropyl) carbodiimide hydrochloride (EDC), Freund's adjuvants, bovine serum albumin (fraction V, BSA), and chemicals for ELISA were purchased from Sigma-Aldrich (Shenshi Huagong, Wuhan). Paraoxon and paraoxon hapten were purchased from Fluka (Sanyi Chemicals, Wuhan). SWNTs prepared by the HiPco process were purchased from Carbon Nanotechnologies Incorporated. The aryldiazonium cations for PEG was custom synthesized by following modified procedures of Bahr et al. [21,22]. Ferrocenedimethylamine (FDMA) was synthesized by literature methods [23]. Paraoxon–BSA was prepared from the corresponding active ester which was added to BSA in 0.1 M $NaHCO_3$ (pH 6.7). The corresponding active ester was prepared by reacting equimolar amounts of paraoxon hapten with NHS and DCC. The product was purified on a silica gel column eluted with chloroform:hexane (1:1). Conjugate paraoxon–BSA was separated from the reactants on Sephadex G-25, and it contains 40 hapten molecules per BSA molecule. All other reagents were used as received. Aqueous solutions were prepared using Mill-Q water (>18 MΩ cm). Phosphate buffered saline (PBS) solutions were 0.15 M NaCl and 0.1 M phosphate buffer, pH 7.3. Phosphate buffer solution for electrochemistry was prepared using 0.1 M buffer containing 0.05 M KCl (pH 7.0).

Atomic force microscopy (AFM) images were taken on GC plates using a Digital Instruments Dimension 3100 scanning probe microscope. All images were acquired in tapping mode using commercial Si cantilevers/tips (Olympus) used at their fundamental resonance frequencies, which typically varied between 275–320 kHz. Flat-bottom polystyrene ELISA highbinding plates were from Costar (Cambridge, MA). ELISA plates were washed with a 96PW microplate washer from Bio-Rad (Hercules, CA), and absorbances were read in dual wavelength mode (450–650 nm) with an Emax microplate reader from Molecular Devices (Sunnyvale, CA).

2.2. Preparation of the shortened SWNTs

Preparation of the cut SWNTs was similar to the procedure from the literature [24]. Purified SWNTs (10 mg) in a 250 mL flat bottom flask containing 40 mL of a 3:1 v/v solution of concentrated sulfuric acid (98%) and concentrated nitric acid (70%) were sonicated in a water bath at 35–40 °C for 4 h. The resultant suspension was then diluted to 200 mL with water. The cut SWNTs were collected on a 0.2 μm pore filter membrane (Millipore) and washed with 10 mM NaOH aqueous solution, followed by Milli-Q water until the pH of the filtrate reached 7.0. The cut SWNTs were then suspended in 10 mL ethanol without the aid of surfactant.

2.3. Preparation of paraoxon monoclonal antibodies IgG

New Zealand white rabbits were used for preparation of antibodies according to the method described by Heldman et al. [25]. The antibodies were raised by intraperitoneal injections of paraoxon hapten conjugated to BSA (2 mg protein emulsified in a complete Freund adjuvant, 1:1). Four booster injections were given at 2–4 weeks intervals. Immune sera were collected 10 days following the last injection. Two antisera were used, each of which was collected from different rabbits. Heated sera were used in this study since heating the sera to 64 °C for 1 h is helpful to increase binding ability of IgG to paraoxon. Stable antibody-producing clones were expanded and cryopreserved in liquid nitrogen. The achieved antibodies were classified as anti-paraoxon IgG which were purified on a small scale directly from late stationary phase culture supernatants by saline precipitation with saturated ammonium sulfate followed by affinity chromatography.

2.4. Preparation of immunosensors interface for the detection of paraoxon

Prior to modification, GC electrodes were polished successively with 1.0, 0.3, and 0.05 μm alumina slurries (alumina: Buehler, Lake Bluff, IL, USA) on microcloth pads (Buehler). The electrodes were thoroughly rinsed and sonicated in Milli-Q water for 1 min between polishing steps. Before modification, the electrodes were dried with a stream of argon. The derivatization of the clean GC electrode with mixed monolayers of 4-aminophenyl/phenyl (GC–Ph-NH_2/Ph) was conducted with in situ generated aryldiazonium

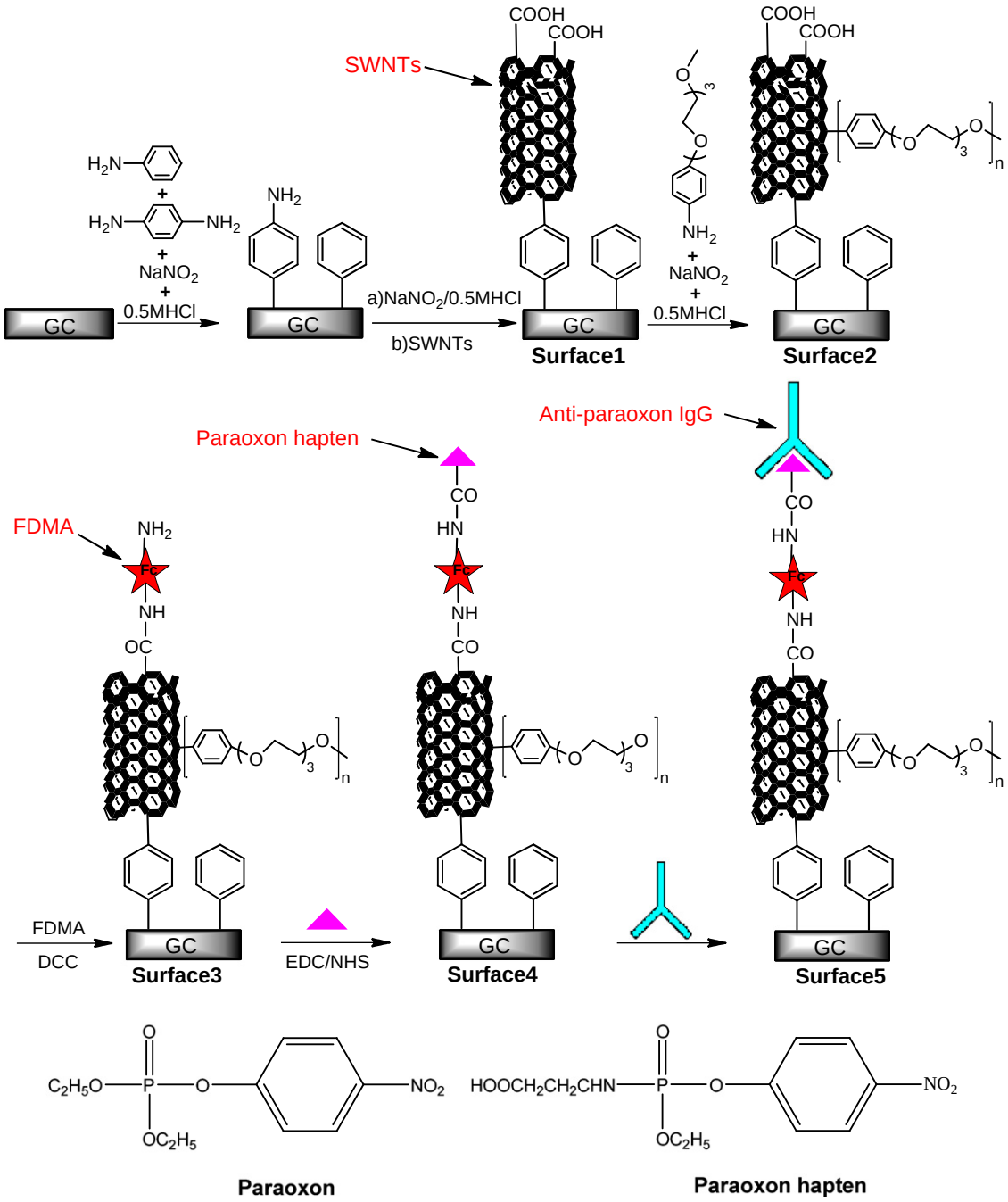

Scheme 1. Schematic of SWNTs modified sensing interface for the detection of paraoxon.

cations involved the electrochemical reduction of the corresponding anilines in acidic media [26,27]. Then the terminal amine groups can be converted to diazonium groups by incubating GC–Ph-NH_2/Ph modified interface in $NaNO_2$ and HCl solution for overnight to form GC–Ph-$N_2^+Cl^-$/Ph as reported in the literature [19]. After surface derivatization, the electrodes were rinsed with copious amounts of Milli-Q water and dried under a stream of argon prior to the next step. The cleaned electrode was immersed in 0.5 mol L^{-1} HCl solution of cut SWNTs (1 mg mL^{-1}) overnight to achieve Surface 1 as shown in Scheme 1. Then Surface 2 was prepared by aryldiazonium treatment of SWNTs reported by Bahr et al. [22]. For coupling FDMA to the open ends of the SWNTs assembled on GC substrates, Surface 2 was incubated in an absolute ethanol solution containing 40 mM DCC and 5 mM FDMA for 6 h at room temperature to achieve Surface 3. Paraoxon hapten was coupled to the ferrocene by immersing the electrodes in 1 mg mL^{-1} hapten in a stirred solution of 20 mM EDC and 4 mM NHS in 0.1 M phosphate buffer (pH 7.0) for 2 h at 4 °C. Surface 4 was rinsed with copious amounts of water and PBS before immersion into a PBS solution of paraoxon monoclonal IgG for 30 min at 4 °C to achieve the sensing interface (Surface 5).

2.5. Electrochemistry measurements

All electrochemical experiments were conducted using GaossUnion EC510 potentiostats. GC electrodes were 3 mm disks embedded in epoxy resin (GaossUnion, Wuhan). All experiments utilized a Pt secondary electrode with Ag/AgCl (3.0 M NaCl) reference electrode. All voltammetric measurements were obtained with the scan rate of 100 mV s^{-1}. All cyclic voltammetry

(CV) and square wave voltammetry (SWV) measurements were carried out in pH 7.0 phosphate buffers.

3. Results and discussions

The CV recorded at GC electrode immersed in solution of the in situ generated diazonium salt mixture of 4-aminophenyl and phenyl shows two irreversible cathodic peaks (peak a and peak b) centered at 0.2 V and −0.45 V (Fig. 1), respectively. During the second cycle, these redox waves disappeared and the CV only exhibits a very small current, which suggests the presence of the grafted layers. The second cathodic peak (peak b) centered at −0.45 V corresponds to the reduction of the aryldiazonium cations to a radical which then binds to the surface. The origin of peak a is not clear, but the observation is consistent with previous reports [28–30].

SWNTs were assembled onto GC–Ph-$N_2^+Cl^-$/Ph modified GC surface by reacting the substrate with cut SWNTs (1 mg mL^{-1}) overnight in 0.5 mol L^{-1} HCl solution. The so-fabricated surface is referred to as Surface 1 and was imaged by AFM as shown in Fig. 2. The AFM results show that the shortened SWNT aligned normal to the electrode surface, and the estimated coverage of SWNTs is 32 pmol cm^{-2} from the AFM images.

As can be seen in Scheme 1, Surface 3 with the terminal amine groups can be modified with paraoxon hapten followed by the immobilization of paraoxon monoclonal antibody IgG through biomolecular affinity to form the sensing interface for the direct detection of paraoxon. The performance of so fabricated immunosensor depends on the affinity between the prepared anti-paraoxon IgG and paraoxon. A competitive indirect ELISA was used for the study of anti-paraoxon IgG sensitivity and specificity to paraoxon. ELISA plates were coated overnight with conjugate or antibody solutions in 50 mM carbonate buffer, pH 9.6. A volume of 100 μL per well was used throughout all assay steps, and all incubations were carried out at room temperature. After each incubation, plates were washed four times with washing solution (0.15 M NaCl containing 0.05% Tween 20). The sensitivity of the plate ELISA for paraoxon (IC_{50}, calculated as the concentration of paraoxon giving 50% inhibition of color development) was $(2.3 \pm 0.4) \times 10^{-5}$ mol L^{-1}. The cross-reactivity toward other organophosphorus pesticides was listed in Table 1. Diethyl phosphate and *p*-nitrophenol have been found to exhibit no cross-reactivities (0.03% and 0.01%, respectively). Parathion, which is structurally related to paraoxon, showed cross-reactivity of 5%. The results are consistent with the previous studies by Heldman et al. [25]. Therefore, the prepared anti-paraoxon IgG were specific for paraoxon without cross-reactivity with *p*-nitrophenol, or diethyl phosphate, and with negligible cross-reactivity with parathion.

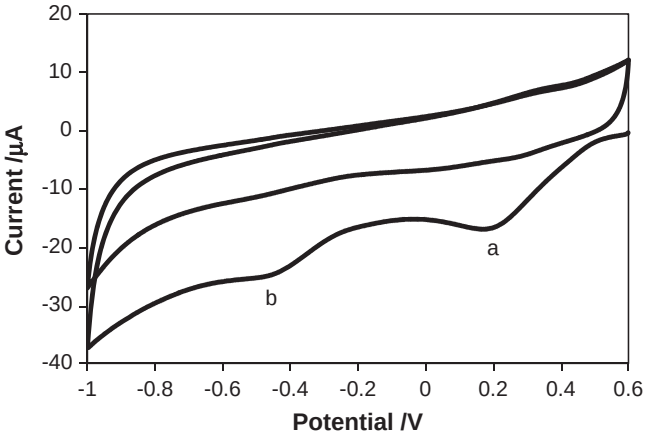

Fig. 1. Cyclic voltammogram at a scan rate of 100 mV s^{-1} for a GC electrode in a solution containing 0.5 mM 4-phenylenediamine, 0.5 mM aniline, and 1 mM $NaNO_2$ in an aqueous medium with 0.5 M HCl as the supporting electrolyte.

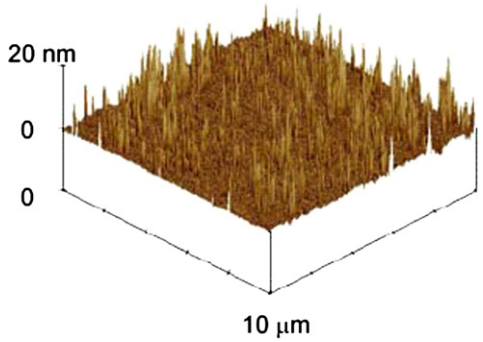

Fig. 2. AFM image of self-assembled SWNTs on GC plate after overnight incubation.

The SW voltammograms, as a more sensitive electrochemical technique, was used to monitor electrochemistry for Surface 3, Surface 4, Surface 5, and Surface 5 after incubation with the analyte paraoxon (Fig. 3). After the attachment of paraoxon hapten, the electrochemistry of GC electrode surfaces showed only minor change in peak currents. This is an encouraging result as it indicates the small molecule epitope does not block the surface electrochemistry, a necessary condition for the sensor to be able to operate. However, electrochemistry of Surface 4 demonstrated pronounced reductions in peak height (decreased by 35 ± 4%) after incubation in paraoxon monoclonal antibody solution. The non-specific adsorption of protein on modified GC surfaces was also assessed. This was determined by incubating of BSA and anti-pig IgG after incubation of paraoxon hapten. Since these two proteins are not specific for paraoxon hapten and any current decrease in these two cases is indicative of non-specific adsorption of protein on the paraoxon hapten modified surface. Very small current decrease (decreased by 0.2 ± 0.02%) was observed. It can therefore be concluded that Surface 2 provides sufficient resistance to non-specific adsorption of protein as reported previously [31]. And it can be confidently concluded that the observed electrochemistry should be assigned to protein attached to the end of the SWNTs as depicted in Scheme 1.

As shown in Fig. 3 incubation of Surface 5 with the analyte paraoxon results in an increase in current, which is consistent with the displacement of anti-paraoxon IgG from the monolayer system to bind with paraoxon in analyte solution resulting in an associated increase in current. In addition, higher concentration of paraoxon and longer incubation time results in higher current increase. These results are consistent with those reported in our previous studies [31,32]. However, the current ($I_{Paraoxon}$ = 0.23 ± 0.08 μA, n = 5) after incubation of the Surface 5 with paraoxon solution is lower than the current ($I_{Paraoxon\ hapten}$ = 0.33 ± 0.04 μA, n = 5) before incubation of the Surface 4 with anti-paraoxon IgG solution. The optimized incubation time is 5 min, and $I_{Paraoxon}$ ($I_{Paraoxon}$ = 70% $I_{Paraoxon\ hapten}$)

Table 1
Selectivity of the anti-paraoxon IgG to organophosphorus pesticides.

Cross-reactivity(%)[a]	Pesticides			
	Paraoxon	*p*-Nitrophenol	Diethyl phosphate	Parathion
Anti-paraoxon IgG	100 ± 5	0.01 ± 0.002	0.03 ± 0.001	5 ± 1

[a] Percentage of cross-reactivity = (IC_{50} of paraoxon/IC_{50} of other compound) × 100. Values correspond to the average of three separate measurements ± standard deviation.

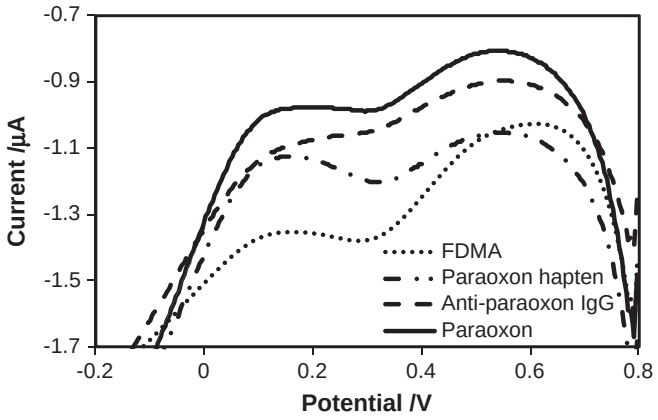

Fig. 3. The example of SWV for SWNTs modified GC electrodes after the stepwise incubation with FDMA, paraoxon hapten, anti-paraoxon IgG, and the analyte paraoxon.

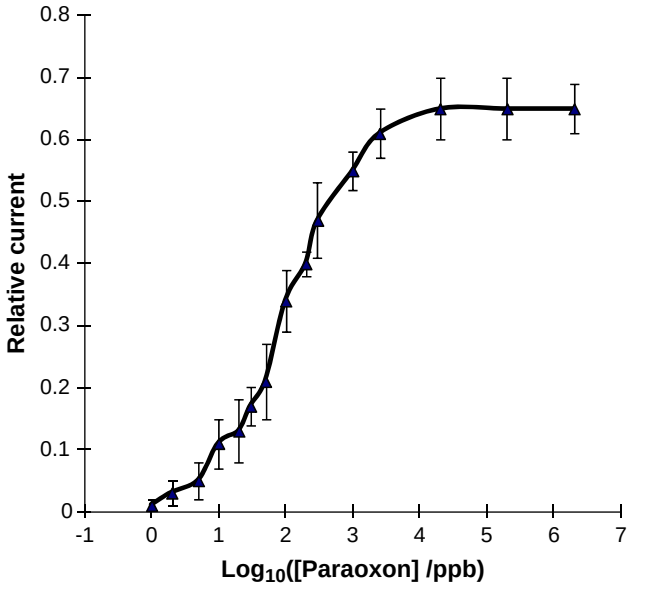

Fig. 4. A calibration curve showing the variation in relative current ($I_{Paraoxon}/I_{Paraoxon\ hapten}$) with the logarithm of the concentration of paraoxon in 0.05 M phosphate buffer (0.05 M KCl, pH 7.0).

is saturated when the concentration of paraoxon is 2500 ppb. It indicates that only 70% anti-paraoxon IgG can dissociate from the interface upon exposure to free paraoxon in solution. The incomplete desorption of anti-paraoxon IgG may be due to the irreversibility of biovalent binding between anti-paraoxon IgG and paraoxon hapten on the interface. The control shows after Surface 5 was exposed to PBS background solution, only a modest increase (1%) in current density was observed possibly due to displacement of weekly bound anti-paraoxon IgG from the surface. Thus the fabricated sensing interface can be used for the detection of paraoxon by a displacement assay. Fig. 4 shows the calibration curve for the detection of free paraoxon in phosphate buffer solution under optimal experimental conditions. This immunosensor allows for detecting paraoxon with the concentration between 2500 ppb and 2 ppb. The detection limit is 2 ppb (2 ng mL_{-1}) which is close to that (1.7 ng mL^{-1}) obtained by the immunochromatographic assay [33], and lower than that (12 ng mL^{-1}) from an electrochemical immunosensor [13]. Under optimal experimental conditions, the displacement assay can provide similar electrochemical signal after six repeated measurements with a relative standard deviation of (6.4 ± 0.3)%. The reproducibility was evaluated by testing and the relative standard deviation of the immunosensor responses of three separately prepared immunosensors were (5.7 ± 0.5)%.

Table 2
Recovery of paraoxon in water samples using the developed immunosensor by a displacement assay.

	Water samples			
	Field water	Lake water	Tap water	Purified water
Recovery(%)[a]	79 ± 6	83 ± 5	92 ± 3	95 ± 4

[a] Values correspond to the average of three separate measurements with ± standard deviation.

The fabricated immunosensor was used for the detection of paraoxon (100 ppb) spiked in four environmental water samples by a displacement assay (Table 2). Field water was collected from a farm, and the lake water was collected from a lake close to a farm. The recovery obtained for paraoxon detection with four paraoxon spiked samples is 79%, 83%, 92%, and 95% respectively. The recovery for field water and lake water was lower than that for tap water and purified water, which might be due to the contaminants from crops and animals in the farm resulting in the matrix sample effect.

4. Conclusions

Herein a label-free immunosensor based on SWNTs modified GC electrodes has been developed for the direct detection of paraoxon. Based on aryldiazonium salt chemistry, forest of SWNTs can be vertically aligned on mixed monolayers of diazonium salts modified GC electrodes by C–C bonding, which provides an interface showing efficient electron transfer between biomolecules. PEG molecules were introduced to the interface to resist non-specific protein adsorption. Then the redox molecules FDMA can be attached to the SWNTs modified interface followed by the attachment of paraoxon hapten and anti-parapxon IgG. This formed sensor system shows good selectivity and high specificity to paraoxon. Based on the change in ferocene current, the immunosensor can be used for the detection of paraoxon in both laboratory and field by a displacement assay. There is a linear relationship between electrochemical signal of FDMA and the concentration of paraoxon over the range of 2–2500 ppb with a lowest detected limit of 2 ppb in 50 mM phosphate buffer at pH 7.0. The developed immunosensing strategy is versatile and attractive for the on-site detection of small molecules in environmental monitoring.

Acknowledgments

This work was financially supported by the National Natural Science Foundation of China (Grant 209237057).

References

[1] M.A. Gallo, N.J. Lawryk, Handbook of Pesticide Technology, second ed., Academic Press, New York, 1991.
[2] J.E. Oliveiraa, V.P. Scagiona, V. Grassia, D.S. Correaa, L.H.C. Mattosoa, Sens. Actuators B 171–172 (2012) 249.
[3] S.P. Sharmaa, L.N.S. Tomara, J. Acharyaa, A. Chaturvedia, M.V.S. Suryanarayana, R. Jain, Sens. Actuators B 166–167 (2012) 616.
[4] X. Gao, G. Tang, X. Su, Biosens. Bioelectron. 36 (2012) 75.
[5] S. Gaberlein, M. Knoll, F. Spener, C. Zaborosch, Analyst 125 (2000) 2274.
[6] V. Sacks, I. Eshkenazi, T. Neufeld, C. Dosoretz, J. Rishpon, Anal. Chem. 72 (2000) 2055.
[7] S.H. Chough, A. Mulchandani, P. Mulchandani, W. Chen, J. Wang, K.R. Rogers, Electroanalysis 14 (2002) 273.
[8] M. Ramanathan, A.L. Simonian, Biosens. Bioelectron. 22 (2007) 3001.

[9] A. Mulchandani, P. Mulchandani, W. Chen, J. Wang, L. Chen, Anal. Chem. 71 (1999) 2246.
[10] J.A. Gabaldon, J.M. Cascales, S. Morais, A. Maquieira, R. Puchades, Food Addit. Contam. 20 (2003) 707.
[11] S. Wang, J. Zhang, Z.Y. Yang, J.P. Wang, Y. Zhang, J. Agric. Food Chem. 53 (2005) 7277.
[12] A. Mulchandani, W. Chen, P. Mulchandani, J. Wang, K.R. Rogers, Biosens. Bioelectron. 16 (2001) 225.
[13] S.Q. Hu, J.W. Xie, Q.H. Xu, K.T. Rong, G.L. Shen, R.Q. Yu, Talanta 61 (2003) 769.
[14] W.B. Choi, E. Bae, D. Kang, S. Chae, B.H. Cheong, J.H. Ko, E.M. Lee, W. Park, Nanotechnology 15 (2004) S512.
[15] L.M. Dai, Smart Mater. Struct. 11 (2002) 645.
[16] J. Li, R. Stevens, L. Delzeit, H.T. Ng, A. Cassell, J. Han, M. Meyyappan, Appl. Phys. Lett. 81 (2002) 910.
[17] D.J. Garrett, B.S. Flavel, J.G. Shapter, K.H.R. Baronian, A.J. Downard, Langmuir 26 (2010) 1848.
[18] J.Q. Liu, A. Chou, W. Rahmat, M.N. Paddon-Row, J.J. Gooding, Electroanalysis 17 (2005) 38.
[19] O.A. de Fuentes, T. Ferri, M. Frasconi, V. Paolini, R. Santucci, Angew. Chem. Int. Ed. 50 (2011) 3457.
[20] G.Z. Liu, T. Bocking, J.J. Gooding, J. Electroanal. Chem. 600 (2007) 335.
[21] G.Z. Liu, J.J. Gooding, Langmuir 22 (2006) 7421.
[22] J.L. Bahr, J. Yang, D.V. Kosynkin, M.J. Bronikowski, R.E. Smalley, J.M. Tour, J. Am. Chem. Soc. 123 (2001) 6536.
[23] F. Ossola, P. Tomasin, F. Benetollo, E. Foresti, P.A. Vigato, Inorg. Chim. Acta 353 (2003) 292.
[24] J. Liu, A.G. Rinzler, H.J. Dai, J.H. Hafner, R.K. Bradley, P.J. Boul, A. Lu, T. Iverson, K. Shelimov, C.B. Huffman, F. Rodriguez-Macias, Y.S. Shon, T.R. Lee, D.T. Colbert, R.E. Smalley, Science 280 (1998) 1253.
[25] E. Heldman, A. Balan, O. Horowits, S. Ben-Zion, M. Torten, FEBS Lett. 180 (1985) 243.
[26] J. Lyskawa, D. Belanger, Chem. Mater. 18 (2006) 4755.
[27] G.Z. Liu, M. Chockalingham, S.M. Khor, A.L. Gui, J.J. Gooding, Electroanalysis 22 (2010) 918.
[28] G.Z. Liu, J.Q. Liu, T.P. Davis, J.J. Gooding, Biosens. Bioelectron. 26 (2011) 3660.
[29] P.A. Brooksby, A.J. Downard, Langmuir 20 (2004) 5038.
[30] S. Baranton, D. Belanger, J. Phys. Chem. B 109 (2005) 24401.
[31] G.Z. Liu, S. Wang, J.Q. Liu, D.D. Song, Anal. Chem. 84 (2012) 3921.
[32] G.Z. Liu, M.N. Paddon-Row, J.J. Gooding, Chem. Commun. (2008) 3870.
[33] C. Liu, Q. Jia, C. Yang, R. Qiao, L. Jing, L. Wang, C. Xu, M. Gao, Anal. Chem. 83 (2011) 8778.